DESIGN OF BATTERY THROUGH STATCOM BASED SYNCHRONIZATION TECHNIQUES - CHARGING STATION TIED FROM PHOTOVOLTAIC ARRAY

G. Supraja.
PG Scholar,
Department of EEE,
JNTU Pulivendula,
suprajaganjikunta@gmail.com

N. Visali.
Professor & HOD,
Department of EEE,
JNTU Pulivendula,
nvisali.eee@jntua.ac.in

Abstract - Battery through STATCOM based on grid synchronization algorithms are of great importance in the control of grid connected power converters, as fast and accurate detection of the grid voltage parameters. If the battery is discharged fully, it cannot be synchronized continuously, to avoid this, in this work it is proposed to charge the battery through Photovoltaic Array. This proposed work is crucial in order to implement synchronization algorithms such as phase locked loops (PLLs) under generic grid conditions. The three advanced Synchronization PLLs are Decoupled Double Synchronous Reference Frame (DDSRF) PLL, Dual Second Order Generalized Integrator (DSOGI) PLL and a PLL based on three phase, Enhanced (3phE) PLL and their performance, will be carried out in MATLAB/SIMULINK.

Keywords: Synchronization, Frequency Estimation, Frequency Locked Loops, Phase Locked Loops, Solar panel, MPPT controllers.

I. INTRODUCTION

Distributed generation systems, ideally, should provide to the grid with an uninterrupted flow of energy [1]-[5]. However, in practice, power systems, especially the distribution systems, have numerous nonlinear loads, which significantly affect the quality of power supplied. As a result of the nonlinear loads, the purity of supply wave form is lost. This ends up producing many power quality problems. Apart from nonlinear loads, some system events, both usual (e.g. capacitor switching, motor starting) and unusual (e.g. faults) could also inflict power quality problems [6], [7].

In faulty conditions [8] to mitigate power quality problems, there are many methods, but the use of a custom power device STATCOM is considered to be the most efficient method. In such conditions sequence components, voltage magnitude and phase can be estimated and power quality phenomenon are reduced by STATCOM dependent synchronization strategies used. In these strategies STATCOM is fed from battery. As battery has discharging problems the synchronization is no possible in different abnormal conditions. To solve this problem in this work, battery is replaced by photovoltaic array is shown in Fig.1.

In this work, three improved and advanced grid synchronization systems are studied and evaluated: The Decoupled Double synchronous reference frame PLL (DDSRF PLL), the Dual Second Order Generalized Integrator PLL (DSOGI PLL) and the Three Phase Enhanced PLL (3phEPLL). Their performance, computational cost and reliability of the amplitude and phase detection of the positive sequence of the voltage, patterns extracted from, which have been reproduced in a real scaled electrical network.

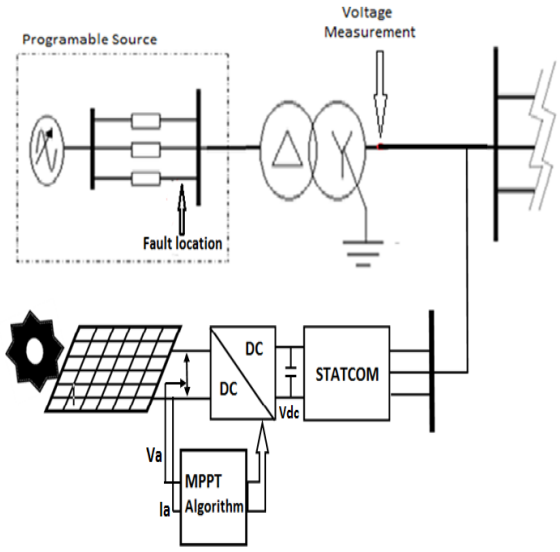

Fig.1. The proposed battery through STATCOM based synchronization techniques - Charging station connected from Photovoltaic Array

II. MODELING OF THE PV ARRAY WITH MPPT ALGORITHM

MPPT algorithms are

- Hill climbing method
- Incremental conductance method

Hill climbing method, predominantly used MPPT method due to no difficulty in execution. Hill climbing strategy outcome has high efficiency [9].

The mathematical models of PV cell current obtained from are as follows:

$$I = N_P I_{ph} - I_D - I_{sh}$$

Here

$$I_{sh} = \frac{V + IR_S}{R_p}$$

$$I_D = N_P I_S \left[e^{\left(\frac{V + IR_S}{\frac{N_S}{nV_t}} \right)} - 1 \right]$$

$$I_{ph} = I_{rr}\left[I_{sc} + (T_{op} - T_{ref})k_i\right]$$

$$I_{rs} = \frac{I_{sc}}{\left[e^{\left(\frac{qV_{oc}}{nkcT_{op}} \right)} - 1 \right]}$$

$$I_S = \left[e^{\left(\frac{1}{T_{op}} - \frac{1}{T_{ref}} \right)\left(\frac{1.12q^2}{nk} \right)} \right] \left[I_{rs} \left(\frac{T_{op}}{T_{ref}} \right)^3 \right]$$

Irradiance (G) = I_{rr} = 500 W/m^2
T_{ref} = 273.15+25 K
T_{op} = 273.15+20 K
$q = 1.6 \times 10^{-19}$ C
Short circuit current (I_{sc}) = 7.2 A
Open circuit voltage (V_{oc}) = 20 V
Short circuit current of temperature coefficient (k_i) = 2.2×10^{-3}
open circuit voltage of temperature coefficient (k_v) = 7.2×10^{-3}
Number of series cells (N_s) = 4
Number of parallel cells (N_p) =1
Series resistance (R_s) = 0.18 ohms
Parallel resistance (R_p) = 360.002 ohms
I_{ro} = 600
Boltzmann constant (K) = $1.38 \times 10^{-23}\ \frac{J}{K}$
Area (n) = 1.36 m^2
Cells in module (c) = 50
Number of modules = 1
Total PV array voltage = 109.091 V
Total PV array current = 1090.91 A
Rating of PV array = 119 KW

III. GRID SYNCHRONIZATION METHODS FOR THREE PHASE DG SYSTEMS

A. *Decoupled Double Synchronous Reference Frame PLL (DDSRF PLL)*

The decoupled double synchronous reference frame [10] is constituted of two rotating reference frames: dq+1, rotating in anticlockwise direction and whose angular position is θ^1, and dq-1, rotating in clock direction and whose angular position is $-\theta^1$. The block diagram of DDSRF PLL is shown in Fig.2.

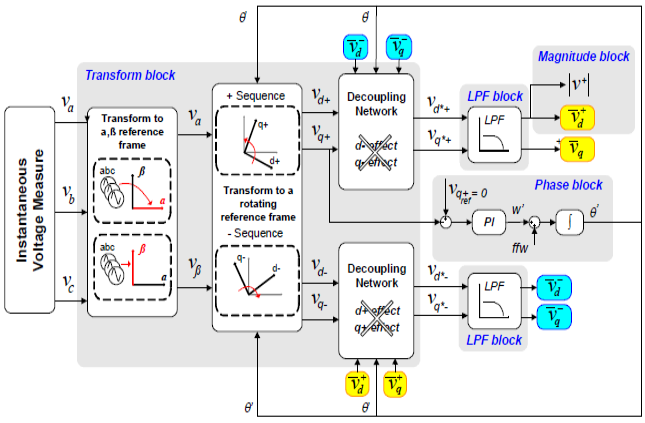

Fig.2. A diagram showing DDSRF PLL

1. *Discrete Implementation*

v_a, v_b, $v_c$are the components of a three phase signal first block in the Fig.2, Clarke's transformation which translates a three phase voltage vector from the abc natural reference frame to the αβ stationary reference frame. The second block is the park's transformation which translates the αβ stationary reference frame to dq rotating frame.

$$\begin{bmatrix} V_\alpha \\ V_\beta \end{bmatrix} = \begin{bmatrix} 1 & -\frac{1}{2} & -\frac{1}{2} \\ 0 & \frac{\sqrt{3}}{2} & -\frac{\sqrt{3}}{2} \end{bmatrix} \begin{bmatrix} V_a \\ V_b \\ V_c \end{bmatrix} \quad \text{Where} \quad \begin{bmatrix} V_a = V\sin(\theta) \\ V_b = V\sin(\theta - 120°) \\ V_c = V\sin(\theta + 120°) \end{bmatrix} \quad (1)$$

$$\begin{bmatrix} V_d \\ V_q \end{bmatrix} = \begin{bmatrix} \cos\theta' & \sin\theta' \\ -\sin\theta' & \cos\theta' \end{bmatrix} \quad (2)$$

a. *Decoupling Networks*

Positive sequence along with negative sequence decoupling networks in equation form represented in (3), (4).

$$\begin{bmatrix} \overline{v_d^+} \\ \overline{v_q^+}^* \end{bmatrix} = \begin{bmatrix} v_d^+ \\ v_q^- \end{bmatrix} - \begin{bmatrix} \cos\theta & \sin\theta \\ -\sin\theta & \cos\theta \end{bmatrix} \begin{bmatrix} \overline{v_d^-}^* \\ \overline{v_q^-}^* \end{bmatrix} \quad (3)$$

$$\begin{bmatrix} \overline{v_d^-}^* \\ \overline{v_q^-}^* \end{bmatrix} = \begin{bmatrix} v_d^+ \\ v_q^- \end{bmatrix} - \begin{bmatrix} \cos\theta & \sin\theta \\ -\sin\theta & \cos\theta \end{bmatrix} \begin{bmatrix} \overline{v_d^+}^* \\ \overline{v_q^+}^* \end{bmatrix} \quad (4)$$

b. *Phase Block Discretization*

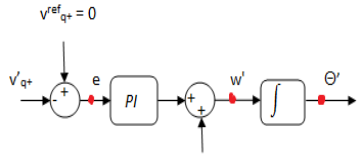

Fig.3. Angle estimation

In the DDSRF PLL the estimation of the angle comes from the integration of the estimated frequency, which corresponds to the output of a PI, as shown in Fig.3.

B. *Dual Second Order Generalized Integrator PLL (DSOGI PLL)*

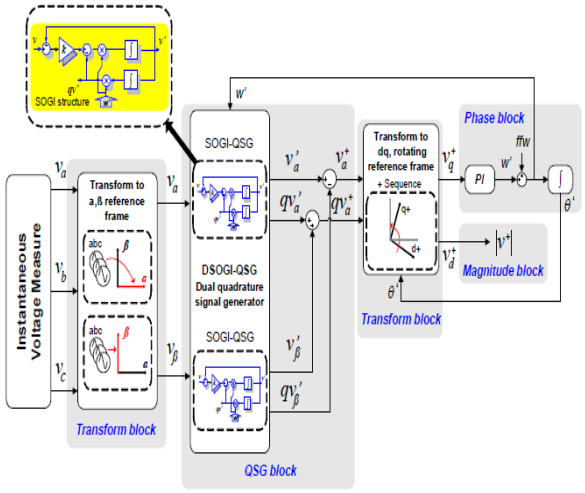

The operating principle of the DSOGI-PLL [11] for estimating the positive and negative-sequence components of the grid voltage vectors is based on using the Instantaneous Symmetrical Components (ISC) method of the αβ stationary reference frame. The diagram of the DSOGI-PLL is shown in Fig.4. As a consequence, the fundamental grid frequency (ω') and the phase-angle of the positive-sequence voltage vector ($\theta^{+'}$) are estimated by this loop. The estimated frequency for the fundamental grid component is fed back to adapt the center frequency, ω', of the DSOGI.

Fig.4. A diagram showing Dual Second Order Generalized Integrator PLL

C. *Three Phase Enhanced PLL (3phEPLL PLL)*

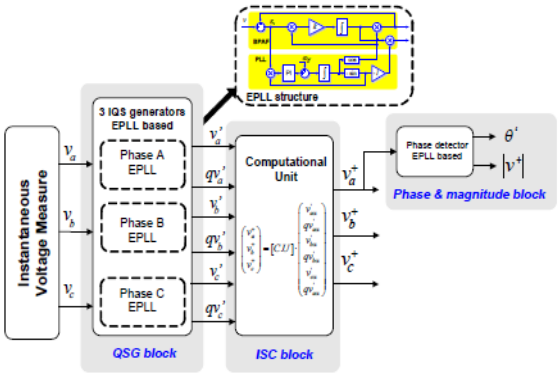

Fig.5. A diagram showing Three Phase Enhanced PLL

Enhanced phase-locked loop is a frequency [12] adaptive nonlinear synchronization approach. The block diagram of EPLL is shown in Fig.5.

EPLL can provide higher degree of immunity and insensitivity to noise, harmonics and unbalance of the input signal. It is an effective method for synchronization of the grid-interfaced converters in polluted and variable frequency environments. In addition, EPLL can provide the 90 degrees shift of the input signal. Therefore, it is an attractive solution in some three phase system applications.

1. *Computational Block Unit*

The description for this block is the same in both discrete and continuous domain. Nevertheless, specific equations are used in this paper, as shown in (5), (6), (7).

$$v_a^+[n] = \frac{1}{3}v_a'[n] - \frac{1}{6}(v_b'[n] + v_c'[n]) + \frac{1}{2\sqrt{3}}(jv_b'[n] - jv_c'[n]) \quad (5)$$

$$v_c^+[n] = \frac{1}{3}v_c'[n] - \frac{1}{6}(v_a'[n] + v_b'[n]) - \frac{1}{2\sqrt{3}}(jv_a'[n] - jv_b'[n]) \quad (6)$$

$$v_b^+[n] = -(v_a^+[n] + v_c^+[n]) \quad (7)$$

2. *QSG Block - EPLL Discretization*

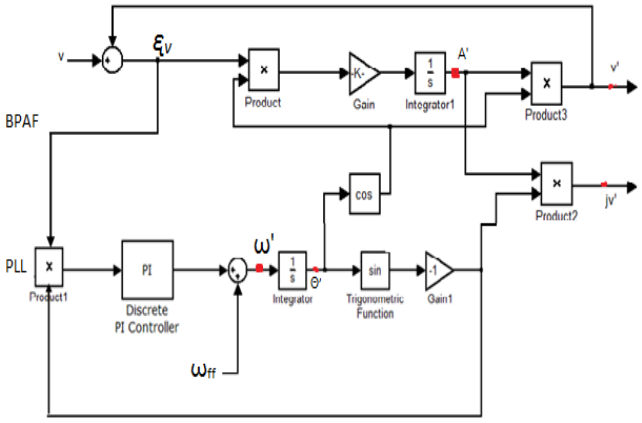

Fig.6. Quadrature Signal Generator based on an Enhanced Phase-Locked Loop structure

IV. SIMULATION RESULTS

In order to obtain the aforementioned sags, different faults are produced with the programmable AC source at the primary winding of the transformer, as indicated in Fig.1.

Depending on the fault topology, as well as on the connection of the transformer, the desired voltage waveforms at the measurement point, indicated in TABLE I. Those values are extracted Three DDSRF PLL, DSOGI PLL and 3phEPLL PLL according to the experimental fault patterns.

In all tests the same pre-fault component has been used:

$$V^+ = 100\angle 0^0, V^- = 0\angle 0^0, V^0 = 0\angle 0^0$$

The fact that the power source is not generating exactly three shifted sine waves, appeal comprehensible, will produce also small negative sequence component in the input. However this slight unbalances also appears in real power systems, accordingly this is not hindering the consistently good in performance of the test.

TABLE I
PROPERTIES OF THE TESTING VOLTAGE SAGS

A Sag	B Sag	C Sag	D sag
$V^+ = 40\angle -40^0$	$V^+ = 73.3\angle -10^0$	$V^+ = 52.74\angle -5.7^0$	$V^+ = 67.37\angle -5.7^0$
$V^- = 0\angle 0^0$	$V^- = 26.6\angle 170^0$	$V^- = 28.52\angle -2.2^0$	$V^- = 27.81\angle -177.8^0$
$V^0 = 0\angle 0^0$	$V^0 = 26.6\angle 170^0$	$V^0 = 0\angle 0^0$	$V^0 = 0\angle 0^0$

Positive, negative and zero sequence vectors during the fault conditions for the different sags

The parameters used for tuning the different advanced synchronization systems analyzed in this work are encapsulated in TABLE II.

TABLE II
TUNING PARAMETERS OF THE ANALYZED PLLS

DDSRF-PLL	DSOGI-PLL	3phEPLL
T_s=100µs	T_s=100µs	T_s=100µs
K_p=2.22	K_p=2.22	K_p=5
K_i=246.74	K_i=61.7	K_i=450
ω_{ff}=314.1592 rad/sec	ω_{ff}=314.1592 rad/sec	ω_{ff}=314.1592 rad/sec
ω_f=157.0796 rad/sec	K=$\sqrt{2}$	K=500

Table III
Number of Manipulations Performed By Each PLL

Structure	A	M	T	S	D
DDSRF PLL	22	32	12	14	0
DSOGI PLL	38	86	4	8	2
3phEPLL	42	41	19	16	0

A=Addition M=Multiplication T=Trigonometric S=variable storage D=Division..

TABLE IV
Execution time estimation

Structure	Execution Time
DDSRF PLL	5.41µs
DSOGI PLL	5.91µs
3PhEPLL	8.36µs

The consequences from TABLE III along with TABLE IV appear ensures that the DDSRF PLL along with DSOGI PLL algorithms are acquires the quick response. On the alternative part, the number of addition, multiplication and trigonometric functions performed by 3phEPLL more and also execution time is high since it is slowest algorithm.

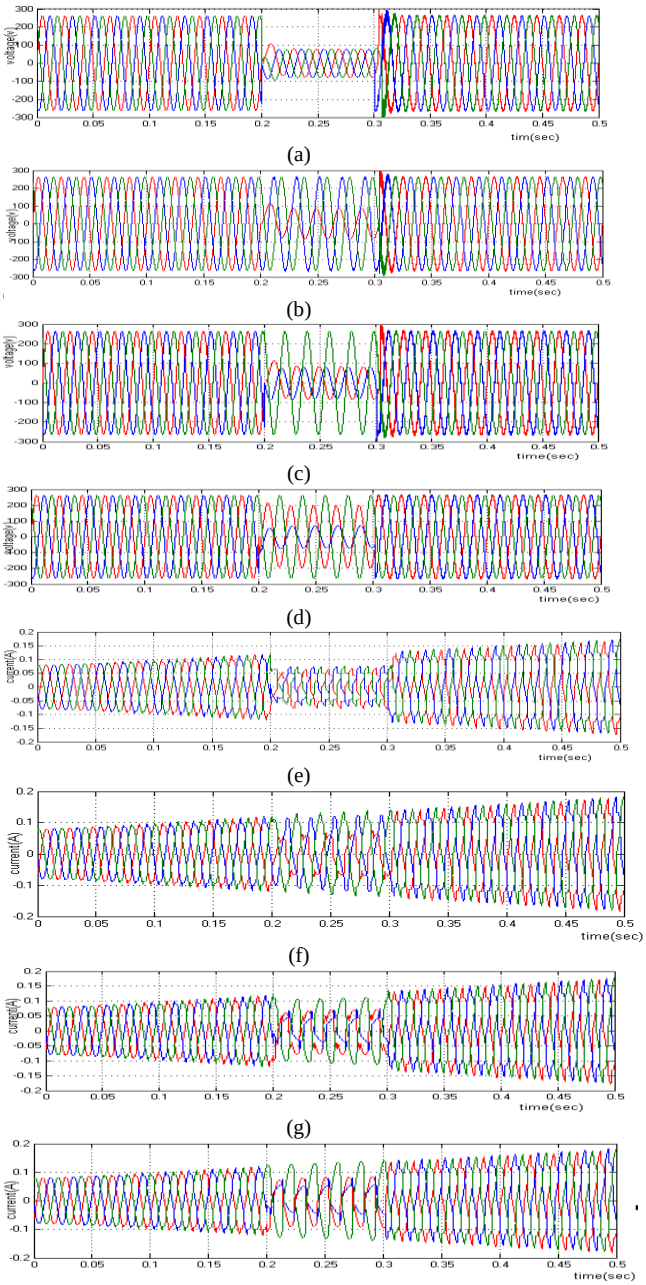

Fig.7. Generation of different types of sags under LLLG, LG, LLG, and LL faults voltage (a)-(d) and current (e)-(h) wave forms without FACTS based PLLs

In this work, voltage sag due to power system faults such as 3-phases-to-ground, phase-to-ground, phase-to-phase-to-ground and phase-to-phase are produced in transmission lines for initiating of dissimilar types of voltage sags are represented in Fig.7. It consisting fault transition time 0.2-0.3s

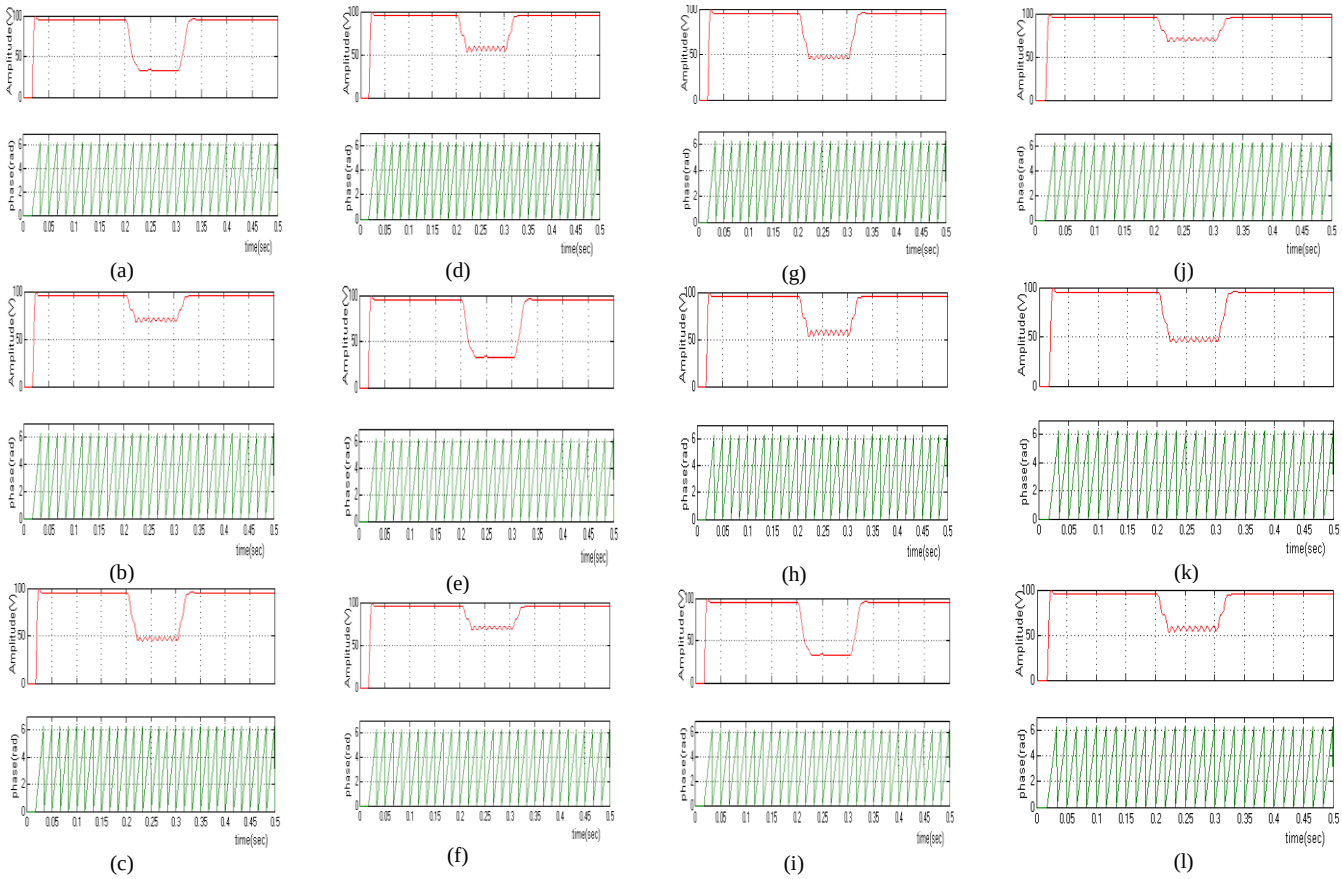

Fig.8. Magnitude and angle evaluation of the three tested PLL's in instant of four kinds of sags. (a) – (d) Magnitude (V) and angle (rad) recognition for the DDSRF PLL; (e) – (h) Magnitude (V) and angle (rad) recognition for the DSOGI PLL; (i) – (l) magnitude (V) and angle (rad) recognition for the 3phEPLL PLL

Positive sequence components for LLLG, LG, LLG, LL faults can be extracted by using DDSRF PLL, DSOGI PLL and 3phEPLL is represented in Fig.8. In this work it will be examine that the estimation of the voltage conditions bring within 20-25ms

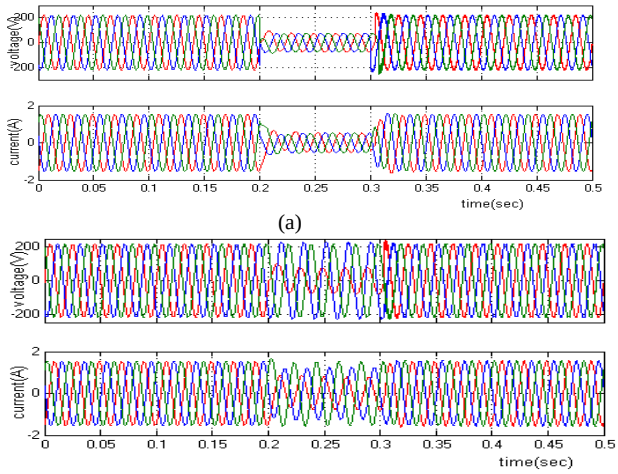

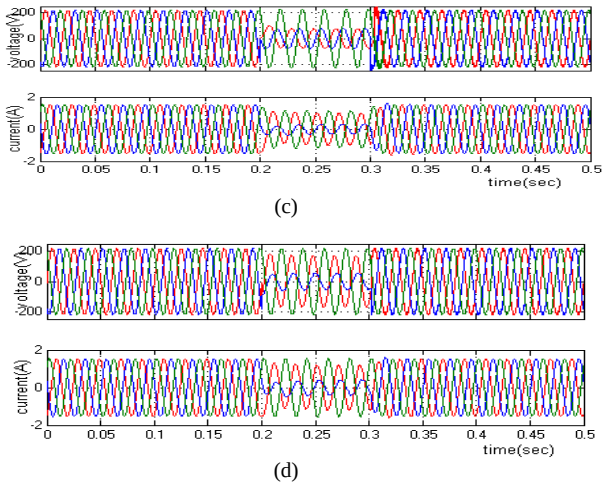

Fig.9. The input signals under different PLLs in different types of sags (a) LLLG Fault (b) LG Fault (c) LLG Fault (d) LL Fault.

Unbalances and distortions occurred in the systems the current drawn by system is not being sinusoidal, even when it is connected to a sinusoidal voltage. These sinusoidal currents contain harmonic

currents that interact with the impedance of the power distribution system to create voltage distortion. By using three phase locked loops these voltage distortions, non linearity's and harmonics in currents are eliminated. This is shown in Fig.9.

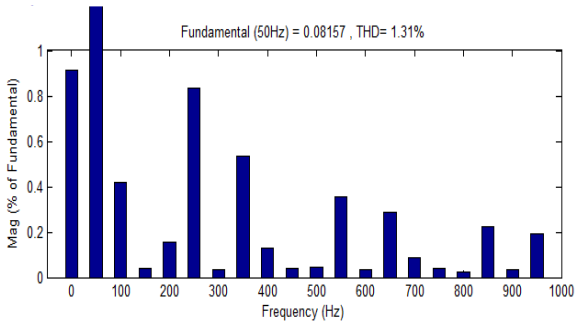

Fig.10. Total harmonic distortion of System without PLLs

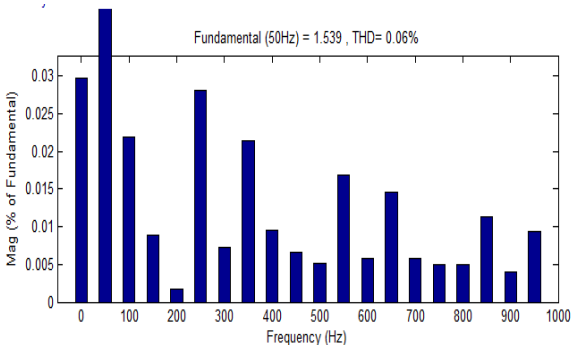

Fig.11. Total harmonic distortion of System with PLLs

The Total harmonic distortion in the system without PLLs is higher than system with PLLs is shown in Fig.10 and Fig.11.

V. CONCLUSION

The three grid synchronization methods are studied in detail in this work. Among the three synchronization techniques the DDSRF-PLL and the DSOGI-PLL use 'αβ' reference frame for the evaluation of the instantaneous symmetrical components of the 3-Ø system, while 3phEPLL uses 'abc' reference frame, working with three variables.

Each of the 3 methods has some merits and demerits when seen individually. But when compared, the DDSRF-PLL has slightly more merits. Due to this it is the best method among the three.

References

[1] BlaabjergF, TeodorescuR .Over view of control and grid synchronization for distributed power generation systems. IEEE TransIndElectron2006;53 (5):1398–409.

[2] Pozzebon GG, GoncalvesAFQ, PenaGG, MocambiqueNEM, Operation of a three phase power converter connected to a distribution system. IEEETransIndElectron2013.

[3] Azadian F, RadziMAM. A general approach toward building integrated photovoltaic systems and its implementation barriers: Areview.RenewSustain Energy Rev2013;22:527–38.

[4] Hosenuzzaman M, RahimNA, SelvarajJ,HasanuzzamanM, MalekABMA, Nahar A.Globa lprospects, progress, policies, and environmental impact of solar photovoltaic power generation. RenewSustainEnergyRev2015;41:284– 97.

[5] PetinrinJO ,ShaabanM. Renewable energy for continuous energy sustain- ability in Malaysia. Renew Sustain Energy Rev2015; 50:967–81.

[6] Dini DH, MandicDP. Widely line a rmodeling for frequency estimation in unbalanced three phase power systems. IEEETransInstrumMeas2013;62 (2):353–63.

[7] Lin J, ChengL, ChangY, ZhangK, ShuB,LiuG. Reliability based power systems planning and operation with wind power integration: Areview to models, algorithms and applications. RenewSustainEnergyRev2014;31:921–34.

[8] Gao S, Mike B. Phase-locked loop for AC systems: analyses and comparisons. In: Proceedings of the 6th IET international conference on power electronics, machines and drives (PEMD 2012); 2012.

[9] Essamudin A. Ebrahim: A Novel Approach of Bacteria-Foraging Optimized Controller for DC Motor andCentrifugal Pump Set Fed from Photo-Voltaic Array,In: Journal of Next Generation Information Technology (JNIT), Volume 6, Number 1, February2015, pp. 21-31.

[10] Rodriguez, P., Pou, J., Bergas, J., Candela, I., Burgos, R. and Boroyevic, D. (2005). "Double synchronous reference frame PLL for power converters control," in Power Electronics Specialists, 2005 IEEE 36th Conference on, pp. 1415–1421.

[11] Yuan, X., Merk, W., Stemmler, H. and Allmeling, J. (2002). Industry Applications, IEEE Transactions on, vol. 38, no. 2, Mar-Apr, pp. 523–532.

[12] ------, (2005). Measurement of harmonics/inter-harmonics of timevarying frequencies," Power Delivery, IEEE Transactions on, vol. 20, no. 1, Jan, pp. 23–31.